

Vapor pressure and thermochemical properties of $ZrCl_4$ for ZrC coating of coated fuel particles

LIU Chao(刘超), LIU Bing(刘兵), SHAO You-lin(邵友林),
LI Zi-qiang(李自强), TANG Chun-he(唐春和)

Institute of Nuclear and New Energy Technology, Tsinghua University, Beijing 100084, China

Abstract: Vapor pressure of zirconium tetrachloride ($ZrCl_4$) under vacuum and an argon pressure of 1×10^5 Pa was measured. The thermochemical changes of $ZrCl_4$ during evaporation were studied by thermogravimetry-differential thermal analysis (TG-DTA), X-ray diffractometry (XRD), scanning electron microscopy (SEM) and energy-dispersive X-ray (EDX) analysis. At the same temperature, vapor pressures of $ZrCl_4$ under vacuum and an argon pressure of 1×10^5 Pa are approximately the same. The vapor pressure exceeds 1×10^5 Pa at 340 °C, which is high enough for ZrC coating of coated fuel particles. $ZrCl_4$ sample is hydrolyzed to some extent to give ZrO_2 and HCl, which however, has little influence on vapor pressure of $ZrCl_4$ at high temperature. No $ZrCl_3$ and Cl_2 are produced by decomposition of $ZrCl_4$ during evaporation, which is confirmed by thermodynamic calculation.

Key words: vapor pressure; thermochemical change; ZrC coating; coated fuel particle

1 Introduction

Zirconium tetrachloride is an important chemical raw material for many applications, such as pigment, waterproofing agent and tanning agent and catalyzer [1–4]. With the development of nuclear energy in the world [5–6], zirconium tetrachloride has also gained important applications in nuclear industry [7–8]. One of the most important applications is to prepare ZrC coating of coated fuel particles for high temperature gas cooled reactor. Several routes [9–15] have been developed to prepare ZrC coating, all of which utilized the reaction of a zirconium halide with a hydrocarbon gas. In these routes, accurate control of flow rate of zirconium source is crucial. $ZrCl_4$ vapor route is an effective method to resolve this problem, in which flow rate of zirconium source can be adjusted by controlling heating temperature of $ZrCl_4$ and flow rate of carrier gas. Thus, the vapor pressure and thermochemical changes of $ZrCl_4$ during evaporation are vital for this application.

In the present study, vapor pressure of $ZrCl_4$ under vacuum and an argon pressure of 1×10^5 Pa were measured and discussed. The thermodynamic change of $ZrCl_4$ during evaporation was analyzed. The phase composition, particle size, morphology and element

contents of $ZrCl_4$ sample were investigated. Finally, reaction mechanism of $ZrCl_4$ during evaporation was studied by thermodynamic calculation.

2 Experimental

2.1 Materials and set-up

Zirconium tetrachloride ($ZrCl_4$, 98% purity) was obtained in Beijing Fine Chemical Co. Ltd., China. Set-up for measuring vapor pressure of $ZrCl_4$ was especially designed due to its high sublimation point (331 °C) and corrosivity. The set-up is mainly composed of controllable crucible resistance furnace, vacuum pump, pressure gauge, stainless steel vaporizer, etc, as shown in Fig. 1.

2.2 Vapor pressure of $ZrCl_4$

Measurement of $ZrCl_4$ vapor pressure under vacuum was as follows. At the first step, vaporizer was vacuumized for 30 min, and then heated at a rate of 5 °C/min up to 340 °C. It was isothermally treatment of 30 min every 20 °C interval and corresponding temperature and pressure were recorded. At the second step, a certain amount of $ZrCl_4$ powder was loaded in the vaporizer, and the subsequent procedure was the same as that at the first step.

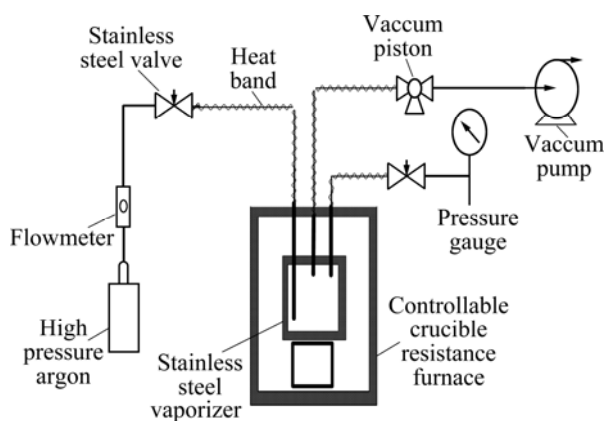


Fig.1 Set-up for measuring vapor pressure of $ZrCl_4$

Measurement of $ZrCl_4$ vapor pressure under an argon pressure of 1×10^5 Pa was as follows. At the first step, vaporizer was vacuumized for 30 min, then argon was introduced to 1×10^5 Pa, and subsequent procedure was the same as that under vacuum.

2.3 Thermochemical change of $ZrCl_4$

The thermodynamic change of $ZrCl_4$ during evaporation was studied by thermogravimetry-differential thermal analysis (TG-DTA, Netzsch STA 449c, Selb, Germany) in an argon atmosphere at a heating rate of $5^\circ C/min$. The composition analyses of $ZrCl_4$ sample before and after evaporation were determined by X-ray diffraction (XRD) pattern from a Guinier-Hägg camera (D/MAX-III B, Rigaku, Tokyo, Japan) with $Cu K_\alpha$ radiation and Si as an internal standard. The particle size, morphology and element contents of $ZrCl_4$ sample before and after evaporation were characterized by a scanning electron microscope (S-3000N, Hitachi, Tokyo, Japan) coupled with an energy dispersive X-ray analysis system (PV7746121 ME, Sapphire, Tokyo, Japan). Finally, the reaction mechanism of $ZrCl_4$ during evaporation was studied by thermodynamic calculation.

3 Results and discussion

Figs.2 and 3 show the vapor pressure of $ZrCl_4$ under vacuum and an argon pressure of 1×10^5 Pa. By considering mixture of gas (or vapor) in vaporizer as ideal gas, the total pressure of mixture in vaporizer is equal to the sum pressure of each gas (or vapor) according to Dalton partial pressure law. So, vapor pressure of $ZrCl_4$ is equal to the pressure difference of the first step and the second step, as shown in Figs.2 and 3.

From Fig.2, between room temperature and $200^\circ C$, vapor pressure of $ZrCl_4$ is very low and there is an obvious increase at about $210^\circ C$. This is because $ZrCl_4$

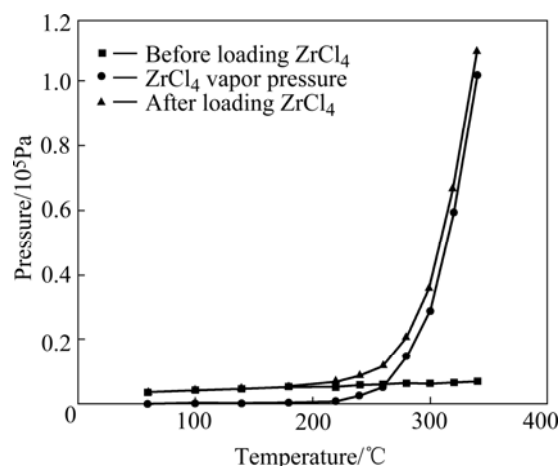


Fig.2 Measurement results of vapor pressure under vacuum

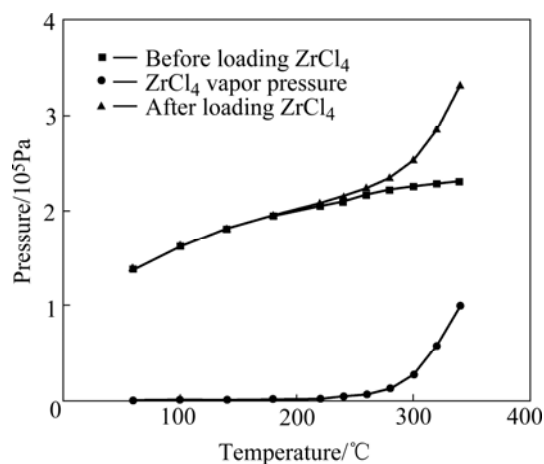


Fig.3 Measurement results of vapor pressure under argon pressure of 1×10^5 Pa

sample is inevitably hydrolyzed to some extent due to absorption of water in air. Hydrolyzing product loses its bonded water and absorbed heat at about $210^\circ C$, which is confirmed by the obvious thermal mass loss in TG curve and the big endothermic peak in DTA curve at $210^\circ C$ (Fig.4). Above $210^\circ C$, vapor pressure increases quickly with the increase of temperature. The higher the temperature is, the quicker the vapor pressure increases. When the temperature reaches $340^\circ C$, vapor pressure pasts 1×10^5 Pa. From the DTA curve, there is a sharp endothermic peak at about $331^\circ C$ with a considerable mass loss in the TG curve. The endothermic peak at $331^\circ C$ is caused by the sublimation of $ZrCl_4$. Pressure between $210^\circ C$ and $331^\circ C$ is mainly caused by $ZrCl_4$ vapor. Besides, there are also some water vapor and chlorine hydride produced by dehydration of $ZrOCl_2 \cdot 8H_2O$.

By considering $ZrCl_4$ vapor, HCl gas and water vapor as ideal gas, the total pressure (p) is linear with temperature (t) when the total molecules (HCl gas, $ZrCl_4$ and water vapor) are constant according to Clapeyron equation:

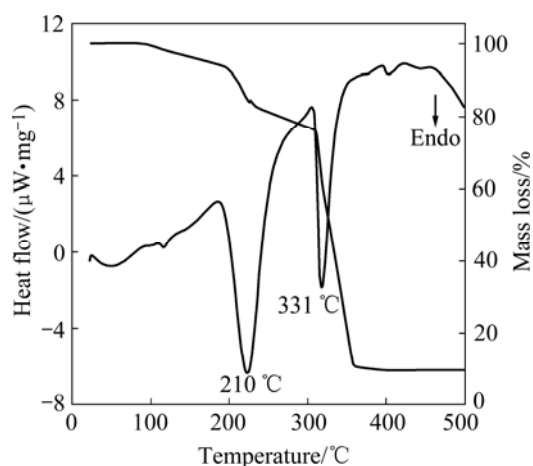


Fig.4 Thermogravimetric and differential thermal analysis curves of $ZrCl_4$

$$pV=nRT \quad (1)$$

where p is pressure; V is volume of gas (or vapor); n is molecules of the gas; R is a constant ($8.314 \text{ J}/(\text{mol}\cdot\text{K})$ for ideal gas) and T is thermodynamic temperature. During evaporation process, molecules of $ZrCl_4$ vapor increase with increasing temperature and finally lead to a quick increase of vapor pressure.

From Fig.3, vapor pressure of $ZrCl_4$ under an argon pressure of $1 \times 10^5 \text{ Pa}$ is similar to that under vacuum and passes $1 \times 10^5 \text{ Pa}$ at about $340 \text{ }^\circ\text{C}$. The similar changes can be found at about $210 \text{ }^\circ\text{C}$ and $340 \text{ }^\circ\text{C}$ as those under vacuum. Thus, it can be concluded that the same reactions happen at above temperatures in both cases.

Comparison of $ZrCl_4$ vapor pressure under vacuum and an argon pressure of $1 \times 10^5 \text{ Pa}$ is shown in Fig.5. It can be seen that the increase rates of $ZrCl_4$ vapor pressure with temperature in both cases are similar. The value under vacuum is a little larger than that under an argon pressure of $1 \times 10^5 \text{ Pa}$ at the same temperature. This is because external pressure makes it difficult for $ZrCl_4$ molecule to escape from zirconium salt.

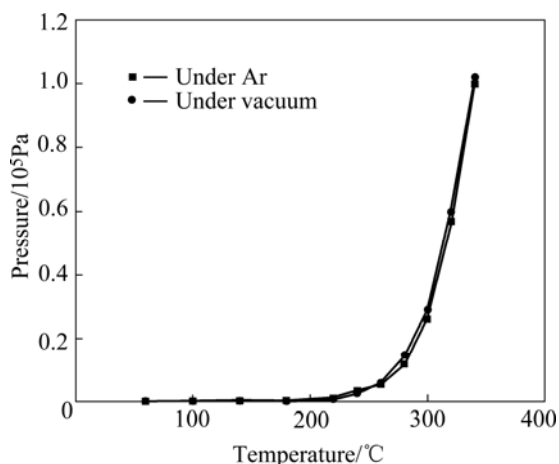


Fig.5 Vapor pressure of $ZrCl_4$ at different temperatures

It is necessary to determine whether vapor pressure satisfies the requests of $ZrCl_4$ vapor route to prepare ZrC coating of coated fuel particles. In terms of typical design parameters of coated fuel particles[16] (Table 1) and optimal process conditions of fluidized bed[17] (Table 2), flow rate of $ZrCl_4$ is calculated to be $4.5 \text{ g}/\text{min}$. Whereas concentration of $ZrCl_4$ vapor at $340 \text{ }^\circ\text{C}$ is calculated to be $4.64 \text{ g}/\text{L}$ by Clapeyron equation. It is easy to satisfy the requests of $ZrCl_4$ vapor route at such high vapor concentration. On the other hand, the concentration of $ZrCl_4$ vapor varies with heating temperature. Thus, flow rate of $ZrCl_4$ can be adjusted by controlling heating temperature of $ZrCl_4$ and flow rate of carrier gas to obtain high performance ZrC coating of coated fuel particles.

Table 1 Typical design parameters of coated fuel particle

Structural item	Size/ μm	Density/ $(\text{g}\cdot\text{cm}^{-3})$
UO_2 kernel	$\Phi^{\textcircled{1}}500$	10.43
Buffer	$d^{\textcircled{2}}95$	1.10
I-PyC	d 40	1.85
ZrC	d 35	6.60

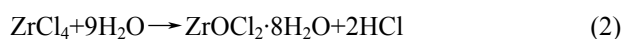
Notes: $\textcircled{1}$ Φ -diameter; $\textcircled{2}$ d - thickness

Table 2 Optimal process conditions of fluidized bed

Status	Flow rate of total gas/ $(\text{L}\cdot\text{h}^{-1})$	Mass of fuel particle/g
Best fluidized	400–800	35

SEM images of $ZrCl_4$ sample before and after evaporation are shown in Fig.6. The particle sizes of $ZrCl_4$ sample before evaporation distribute over $1\text{--}3 \mu\text{m}$ with spherical morphology and white color. After evaporation the particle appears to be in irregular shape with a size of $4\text{--}7 \mu\text{m}$, grey color and several agglomerations. The observations in two images indicate that the composition of $ZrCl_4$ sample before and after evaporation is changed. EDX semi-quantitative analysis results show that the ratio of Zr to Cl of $ZrCl_4$ sample before evaporation is close to 1:4, and the ratio of Zr to O is close to 1:2 after evaporation. The result further indicates that the main composition of sample changes from $ZrCl_4$ to ZrO_2 .

Fig.7 shows the XRD patterns of $ZrCl_4$ sample before and after evaporation, respectively. Only three small diffraction peaks appear in Fig.7(a), which correspond to $ZrCl_4$. There are several sharp diffraction peaks in Fig.7(b) corresponding to monoclinic ZrO_2 ($2\theta=28.180^\circ, 31.468^\circ, 34.147^\circ$) and tetragonal ZrO_2 ($2\theta=30.244^\circ, 50.250^\circ, 60.259^\circ$). ZrO_2 is hydrolyzation product of $ZrCl_4$ via following reactions:



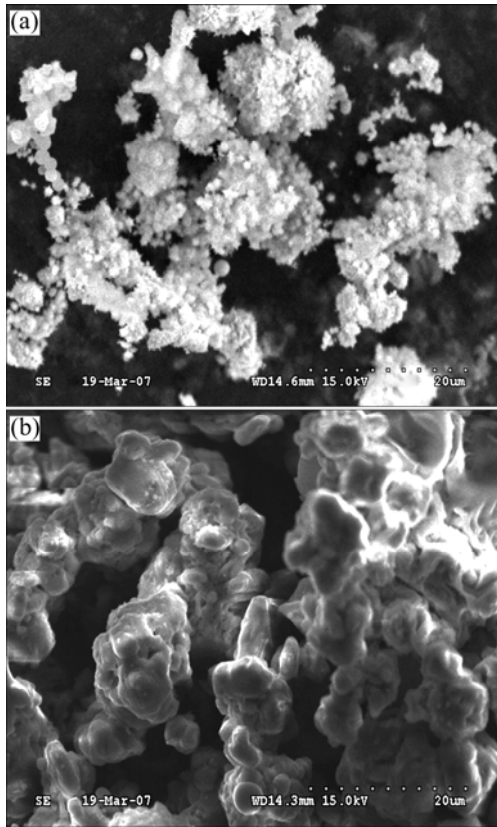


Fig.6 SEM images of ZrCl₄ sample before(a) and after(b) evaporation

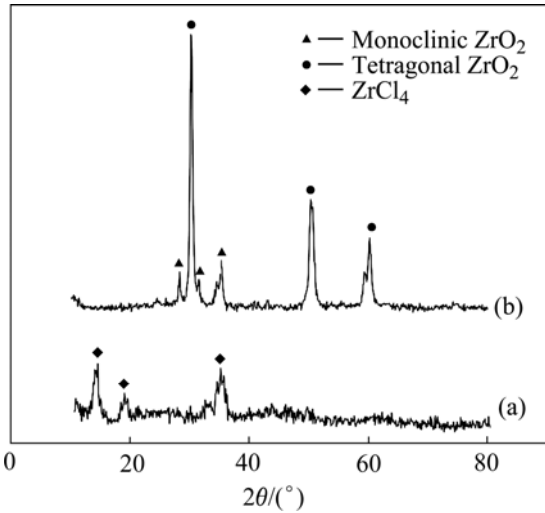
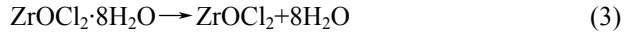


Fig.7 XRD patterns of ZrCl₄ sample before(a) and after(b) evaporation



ZrCl₄ sample is hydrolyzed to some extent. However, the amount is so small that it almost has no influence on vapor pressure of ZrCl₄ at high temperature, which can also be seen from the remaining quantity of ZrCl₄ sample after evaporation. It should be noted that a considerable mass loss appears at about 210 °C corresponding to the dehydration of ZrOCl₂·8H₂O in Fig.4. This is because ZrCl₄ sample in TG measurement is very little and has large specific contact area with argon, which is different from actual evaporation process. So some measurements could be taken to obtain high performance ZrC coating during evaporation of ZrCl₄, such as pumping for a few minutes at about 210 °C to remove HCl and H₂O in ZrCl₄ vapor.

No zirconium halide phases, such as ZrCl₃ and ZrCl₂, are found in Fig.7, indicating that no decomposition of ZrCl₄ happens during evaporation by following reactions:



We can factually discuss the probability of reactions (5) and (6) in temperature range of evaporation by thermodynamic calculation. The main thermodynamic parameters are listed in Table 3. For reaction (5), if it happens in standard state (1×10⁵ Pa, 298.15 K), the Gibbs energy change is

$$\begin{aligned} \Delta_r G^\ominus &= \sum(\Delta_f G^\ominus)_{\text{product}} - \sum(\Delta_f G^\ominus)_{\text{reactant}} = \\ &2\Delta_f G^\ominus[\text{ZrCl}_3] + \Delta_f G^\ominus[\text{Cl}_2] - 2\Delta_f G^\ominus[\text{ZrCl}_4] = \\ &4.88 \text{ kJ/mol} > 0 \end{aligned} \quad (7)$$

If it happens at 1×10⁵ Pa and T, the Gibbs energy change is

$$\Delta_r G_T^\ominus = \Delta_r H_T^\ominus - T\Delta_r S_T^\ominus \quad (8)$$

Enthalpy change ΔH_T^\ominus and entropy change $\Delta_r S_T^\ominus$ can be presented by

$$\Delta_r H_T^\ominus = \Delta_r H^\ominus + \int_{298.15\text{K}}^T \sum \gamma_B c_p^T(B) dT \quad (9)$$

$$\Delta_r S_T^\ominus = \Delta_r S^\ominus + \int_{298.15\text{K}}^T \sum \frac{\gamma_B c_p^T(B) dT}{T} \quad (10)$$

Table 3 Thermodynamic parameters of some substance[18]

Substance	$\Delta_f H^\ominus / (\text{kJ} \cdot \text{mol}^{-1})$	$\Delta_f G^\ominus / (\text{kJ} \cdot \text{mol}^{-1})$	$S^\ominus / (\text{J} \cdot \text{K}^{-1} \cdot \text{mol}^{-1})$	$c_p^\ominus / (\text{J} \cdot \text{K}^{-1} \cdot \text{mol}^{-1})$	A_1	A_2	A_3
ZrCl ₄	-981	-890	181.4	119.8	125.0	14.1	-8.4
ZrCl ₃	-714	-646	146.0	96.0	99.8	12.6	-6.6
ZrCl ₂	-502	-386	110.0	72.6	68.2	18.4	0
Cl ₂	0	0	233.1	33.95	36.9	0.3	-2.8

where $\Delta_r H^\ominus$ and $\Delta_r S^\ominus$ can be calculated:

$$\begin{aligned} \Delta_r H^\ominus &= \sum(\Delta_f H^\ominus)_{\text{product}} - \sum(\Delta_f H^\ominus)_{\text{reactant}} = \\ &2\Delta_f H^\ominus[\text{ZrCl}_3] + \Delta_f H^\ominus[\text{Cl}_2] - 2\Delta_f H^\ominus[\text{ZrCl}_4] = \\ &534 \text{ kJ/mol} \end{aligned} \quad (11)$$

$$\begin{aligned} \Delta_r S^\ominus &= \sum(\Delta_f S^\ominus)_{\text{product}} - \sum(\Delta_f S^\ominus)_{\text{reactant}} = \\ &2\Delta_f S^\ominus[\text{ZrCl}_3] + \Delta_f S^\ominus[\text{Cl}_2] - 2\Delta_f S^\ominus[\text{ZrCl}_4] = \\ &162 \text{ J/(K}\cdot\text{mol)} \end{aligned} \quad (12)$$

c_p^T is determined by A_1, A_2 and A_3 :

$$c_p^T = A_1 + A_2 \times 10^{-3} T + A_3 \times 10^{-5} T^{-2} \quad (13)$$

After integration of reactions (8)–(13), the Gibbs energy change for reaction (5) at 753.15 K is

$$\begin{aligned} \Delta_r G_T^\ominus &= \Delta_r H_T^\ominus - T\Delta_r S_T^\ominus = \\ &537.98 + (13.36T \ln T + 1.39 \times 10^{-3} T^2 - \\ &252.58T - 0.359T^{-1}) \times 10^{-3} = \\ &415.19 \text{ kJ/mol} > 0 \end{aligned} \quad (14)$$

From Eqns.(7) and (14), it can be seen that Gibbs energy change between 298.15 K and 753.15 K is above zero, which indicates that the reaction (5) will not happen spontaneously during evaporation.

The same as above calculations, the Gibbs energy changes of reaction (6) at 298.15 K and 753.15 K are shown as follows:

$$\Delta_r G^\ominus = 1008 \text{ kJ/mol} > 0 \quad (15)$$

$$\Delta_r G_T^\ominus = \Delta_r H_T^\ominus - T\Delta_r S_T^\ominus = 537.48 \text{ kJ/mol} > 0 \quad (16)$$

Obviously reaction (6) will not happen spontaneously during vaporization, either.

4 Conclusions

1) Vapor pressure of ZrCl_4 at 340 °C under vacuum and an argon pressure of 1×10^5 Pa exceeds 1×10^5 Pa, which can satisfy the requests of ZrCl_4 vapor route for preparing ZrC coating of coated fuel particles.

2) Flow rate of ZrCl_4 can be precisely adjusted by controlling heating temperature of ZrCl_4 and flow rate of carrier gas.

3) ZrCl_4 sample is hydrolyzed to some extent to give ZrO_2 and HCl during evaporation, which however, has little influence on vapor pressure of ZrCl_4 at high temperature. According to thermochemical properties of ZrCl_4 during evaporation, some measurements could be taken to obtain high performance ZrC coating.

4) Both experimental and thermodynamic calculation results suggest that ZrCl_4 doesn't decompose to give ZrCl_3 and Cl_2 during evaporation.

References

- [1] Editing Committee of Rare Metals. Handbook of rare metals [M]. Beijing: Metallurgical Industry Press, 1992: 274–280. (in Chinese)
- [2] KUMAR V, KAUR S, KUMAR S. ZrCl_4 catalyzed highly selective and efficient michael addition of heterocyclic enamines with α, β -unsaturated olefins [J]. Tetrahedron Letters, 2006, 47(39): 7001–7005.
- [3] BABU K S, RAJU B C, SRINIVAS P V. Highly efficient and chemoselective cleavage of prenyl ethers using $\text{ZrCl}_4/\text{NaBH}_4$ [J]. Tetrahedron Letters, 2003, 44(12): 2525–2528.
- [4] SMITHA G, REDDY C S. ZrCl_4 -catalyzed aza-michael addition of carbamates to enones: Synthesis of Cbz-protected β -amino ketones [J]. Catalysis Communications, 2007, 8(3): 434–436.
- [5] WANG Ge-hua. Energy and sustainable development [M]. Beijing: Chemical Industry Press, 2005: 26–30. (in Chinese)
- [6] MA Xu-quan. Development and application of nuclear energy [M]. Beijing: Chemical Industry Press, 2005: 6–23. (in Chinese)
- [7] VENKATESH C, VADAKKAPATTU, LEE T W. Multi-dimensional simulations of the chemical vapor deposition for thermal barrier coatings using $\text{ZrCl}_4\text{-H}_2\text{-CO}_2\text{-Ar}$ gas mixtures [J]. Surface and Coatings Technology, 2006, 201(3/4): 1065–1073.
- [8] SAKAMURA Y, INOUE T, IWAI T. Chlorination of UO_2 , PuO_2 and rare earth oxides using ZrCl_4 in LiCl-KCl eutectic melt [J]. Journal of Nuclear Materials, 2005, 340(1): 39–51.
- [9] REYNOLDS G H. Chemical vapor deposition of ZrC on pyrocarbon-coated fuel particles [J]. J Nucl Mater, 1974, 50(2): 215–216.
- [10] IKAWA K, IWAMOTO K. Coating microspheres with zirconium carbide [J]. J Nucl Mater, 1972, 45(1): 67–68.
- [11] IKAWA K, IWAMOTO K. Coating microspheres with zirconium carbide-carbon alloy by iodide process [J]. J Nucl Sci and Tech, 1974, 11(6): 263–267.
- [12] REYNOLDS G H. Chemical vapor deposition of isotropic carbon-zirconium carbide particle coatings [J]. J Nucl Mater, 1975, 56(2): 239–242.
- [13] HOLLABAUGH C M. A new method for coating microspheres with zirconium carbide and zirconium carbide-carbon graded coats [J]. J Nucl Mater, 1975, 57(3): 325–326.
- [14] WALLACE T C. Chemical vapor deposition of ZrC in small bore carbon-composite tubes [J]. Chemical Vapor Deposition, 1973, 4: 91–106.
- [15] IKAWA K, IWAMOTO K. Coating microspheres with zirconium carbide-carbon alloy [J]. J Nucl Mater, 1974, 52(1): 128–130.
- [16] TANG Chun-he, TANG Ya-ping. Design and manufacture of the fuel element for the 10MW high temperature gas-cooled reactor [J]. Nucl Eng Des, 2002, 218: 91–102.
- [17] LI Qi-ming. Chemical vapor deposition of composite gradient coatings for coated fuel particles [D]. Beijing: Tsinghua University, 2000. (in Chinese)
- [18] DEAN J A. Lange's handbook of chemistry [M]. New York, USA: McGraw-Hill Education Co., 1921: 6.142–6.148.

(Edited by LI Xiang-qun)